Molecular and Cellular Biochemistry
https://doi.org/10.1007/s11010-024-05117-7

Sacubitril/valsartan attenuated myocardial inflammation, fibrosis, apoptosis and promoted autophagy in doxorubicin-induced cardiotoxicity mice via regulating the AMPKα–mTORC1 signaling pathway

Feng Hu[1] · Senbo Yan[1] · Li Lin[1] · Xiaoxia Qiu[1] · Xinghe Lin[1] · Weiwei Wang[1]

Received: 19 June 2024 / Accepted: 6 September 2024

Abstract
This study aimed to investigate the potential cardioprotective effects of sacubitril/valsartan (Sac/Val) in mice with doxorubicin (DOX)-induced cardiomyopathy, a common manifestation of cancer therapy-related cardiac dysfunction (CTRCD) associated with DOX. A total of thirty-two mice were equally classified into 4 groups: control group, DOX (total 24 mg/kg), Sac/Val (80 mg/kg), and Sac/Val + DOX (Sac/Val was given from seven days before doxorubicin administration). Neonatal rat ventricular myocytes was exposed to 5 μM of DOX for 6 h in vitro to mimic the in vivo conditions. A variety of techniques were used to investigate cardiac inflammation, fibrosis, apoptosis, and autophagy, including western blot, real-time quantitative PCR (RT-qPCR), immunohistochemistry, and fluorescence. Mice with DOX-induced cardiotoxicity displayed impaired systolic and diastolic function, characterized by elevated levels of cardiac inflammation, fibrosis, cardiomyocyte hypertrophy, apoptosis, and autophagy inhibition in the heart. Treatment with Sac/Val partially reversed these effects. In comparison to the control group, the protein expression of NLRP3, caspase-1, collagen I, Bax, cleaved caspase-3, and P62 were significantly increased, while the protein expression of Bcl-2 and LC3-II were significantly decreased in the myocardial tissues of the Dox-induced cardiomyopathy group. The administration of Sac/Val demonstrated the potential to partially reverse alterations in protein expression within the myocardium of mice with DOX-induced cardiotoxicity by modulating the AMPKα–mTORC1 signaling pathway and suppressing oxidative stress. Additionally, Sac/Val treatment may mitigate Dox-induced apoptosis and inhibition of autophagy in primary cardiomyocytes. Sac/Val seems to be cardioprotective against DOX-induced cardiotoxicity in the pre-treatment mice model. These findings could be attributed to the anti-inflammatory, antioxidant, anti-apoptotic, and de-autophagy effects of Sac/Val through regulation of the AMPKα–mTORC1 signaling pathway.

Keywords Doxorubicin · Cardiotoxicity · Sacubitril/valsartan · Apoptosis

Introduction

Recent advancements in targeted therapies and enhanced screening techniques have shown promising results in improving cancer prognosis. Despite the effectiveness of anthracycline chemotherapy as a fundamental component of cancer treatment, its utilization has been associated with a higher incidence of cancer therapy-related cardiac dysfunction (CTRCD), characterized by a significant decrease in left ventricular ejection fraction (LVEF) of at least 10% or a reduction in LVEF to less than 50% [1].

In a study involving 2625 patients who received anthracycline treatment, with a median follow-up time of 5.2 years post-chemotherapy, the incidence of chemotherapy-related

Feng Hu, Senbo Yan, and Li Lin contributed to this study equally.

✉ Xinghe Lin
291876067@qq.com

✉ Weiwei Wang
weiweiwagn@126.com

[1] Department of Cardiology, Fujian Medical University Union Hospital, Fujian Cardiovascular Medical Center, Fujian Institute of Coronary Artery Disease, Fujian Cardiovascular Research Center, Fuzhou 350001, People's Republic of China

Published online: 20 September 2024

cardiac dysfunction was found to be 9% [2]. Among a total of 12,500 breast cancer patients, the cumulative rates of CTRCD at the first and fifth years were 1.20% and 4.30%, respectively, in patients treated with anthracycline alone, as opposed to 6.20% and 20.10%, respectively, in patients who received a combination regimen of anthracycline and trastuzumab [3]. According to a retrospective study enrolled, a total of 475 breast cancer patients with a median follow-up time of 2.88 years, the incidence of CTRCD was 3.2%, corresponding to an incidence rate of 11.1 per 1000 person-years [4]. The incidence of CTRCD was consistently high in patients receiving combination anthracyclines trastuzumab regimens [4].

Myocardial ultrastructural abnormalities, accompanied by irreversible cardiac dysfunction, were identified as the predominant evidence of anthracycline-induced cardiotoxicity. The main mechanism underlying this phenomenon was attributed to oxidative stress damage [5]. Anthracycline disrupted the normal catalytic cycle of topoisomerase 2-β (Top2β), causing deoxyribonucleic acid double-stranded breaks [5]. It changed the transcriptome, leading to mitochondrial dysfunction, the generation of reactive oxygen species, and subsequent lipid peroxidation of cell membranes [5]. As a result, cardiomyocytes showed myofibrillar disarray and vacuolization [5]. Over the past six decades since the discovery of anthracyclines, significant attention has been devoted to basic science and clinical trials research investigating both its antitumor effects and cardiotoxic mechanisms.

A study found that sixty-four percent of patients with chemotherapy-related cardiotoxicity who were treated with anthracyclines and initiated therapy with enalapril and carvedilol within 1–2 months of detecting LVEF impairment (biplane method according to modified Simpson's rule) experienced complete or partial recovery, in contrast to a lack of response when treatment was delayed until 6 months later [6]. Patients with heart failure and reduced ejection fraction (HFrEF) have significantly benefited from the introduction of angiotensin receptor–neprilysin inhibitor (ARNI).

The distinctive dual neuroendocrine regulatory mechanism of sacubitril/valsartan (Sac/Val) was characterized by the inhibition of neprilysin by LBQ657, which leads to the augmentation of natriuretic peptide levels, and the inhibition of the renin–angiotensin–aldosterone system by valsartan through the blockade of angiotensin II type 1 receptors (AT1R) [7–9]. The AT1R was a G-protein-coupled receptor that endogenously binds to the peptide ligand angiotensin II and activated vasoconstrictor and mitogenic signal transduction pathways resulting in peripheral arteriolar vasoconstriction and increased renal tubular reabsorption of sodium and water [7–9]. Sac/Val showed effectiveness in the management of individuals with ventricular dysfunction and cardiovascular diseases. In comparison to angiotensin-converting enzyme inhibitors (ACEIs), Sac/Val has demonstrated superior efficacy in reducing cardiovascular mortality and hospitalizations due to heart failure in patients with heart failure [8]. Although cancer patients were not excluded "a priori" from enrollment in the pivotal PARADIGM-HF trial (where patient could be enrolled after 12 or more months due to cardiac toxicity), investigators ultimately decided not to enroll these patients [9]. Patients with anthracycline-related cardiomyopathy who were treated with Sac/Val showed improvements in cardiac function and NT-proBNP levels, consistent with the findings from previous observational studies [10].

Despite being derived from small observational studies, Sac/Val improved the clinical symptomatic status, cardiac structure, and function in patients with doxorubicin (DOX)-induced cardiotoxicity [11–15]. Although the demonstration of a beneficial effect of sacubitril/valsartan on CTRCD is promising, the conclusions of these small observational studies remained solely speculative in cancer survivors. Therefore, large-scale prospective clinical studies are required to confirm the performance, and basic experiments are needed to explore the potential molecular mechanisms of ARNI for the prevention and treatment of CTRCD. In this study, we aimed to investigate whether prophylactic treatment with Sac/Val could preserve cardiac function in a mouse model (cumulative doses of DOX have been shown to cause cardiotoxicity [16–18]) of Dox-induced cardiomyopathy through modulation of the AMPK–mTORC1 signaling pathway.

Materials and methods

Ethics statements

In this study, male C57BL/6N mice were purchased from Beijing Vital River Laboratory Animal Technology Co., Ltd (Beijing, China). To rule out the effects of estrogen, we did not taken female mice for molding. All animal experiments were conducted in accordance with the National Institutes of Health (NIH) policies outlined in the Guide for the Care and Use of Laboratory Animals and were approved by the Animal Care and Use Committee of Fujian Medical University Union Hospital (2024KJT011).

Mice model of DOX-induced cardiomyopathy

Doxorubicin hydrochloride was purchased from Sigma-Aldrich (#D1515) and Sac/Val complex was purchased from Novartis Pharma AG Co., Ltd. Thirty-two mice were randomly divided into four groups ($n = 8$) as shown in Table 1; the phosphate buffer saline (PBS); Saline group (CONTROL), PBS; Sac/Val group (Sac/Val), DOX; Saline group (DOX), and DOX; Sac/Val group (Sac/Val + DOX). The mice in the CONTROL and DOX

Table 1 Study protocol

Groups	1–6th day	7th day	8–13th day	14th day	15–20th day	21st day	22–42nd day
PBS; Saline group	Saline (PO)	Saline (PO) PBS (IP)	Saline (PO)	Saline (PO) PBS (IP)	Saline (PO)	Saline (PO) PBS (IP)	Saline (PO)
PBS; Sac/Val group	Sac/Val (PO)	Saline (PO) PBS (IP)	Sac/Val (PO)	Saline (PO) PBS (IP)	Sac/Val (PO)	Saline (PO) PBS (IP)	Sac/Val (PO)
DOX; Saline group	Saline (PO)	Saline (PO) Doxorubicin (IP)	Saline (PO)	Saline (PO) Doxorubicin (IP)	Saline (PO)	Saline (PO) Doxorubicin (IP)	Saline (PO)
DOX; Sac/Val group	Sac/Val (PO)	Saline (PO) Doxorubicin (IP)	Sac/Val (PO)	Saline (PO) Doxorubicin (IP)	Sac/Val (PO)	Saline (PO) Doxorubicin (IP)	Sac/Val (PO)

Doses of treatment: 0.9% saline PO; Sac/Val PO (80 mg/kg); doxorubicin IP [8 mg/(kg.wk)]

DOX doxorubicin, *IP* intraperitoneal, *PO* perioral, *Sac/Val* sacubitril/valsartan

groups were administered an equal volume of perioral 0.9% saline for 42 days. The mice in the Sac/Val and Sac/Val + DOX groups were administered perioral Sac/Val (80 mg/kg sacubitril + valsartan 1/1 complex) [12] in 0.9% saline by gavage for 42 days. On the seventh, fourteenth, 21st day in the DOX and Sac/Val + DOX group, one hour after the perioral saline administration, single-dose intraperitoneal (IP) Dox [8 mg/(kg.wk)] was administered [16]. In mouse chronic heart failure in vivo models, cumulative doses of DOX up to 24 mg/kg have been shown to cause left ventricular systolic dysfunction [16–18]. Correspondingly, on the seventh, fourteenth, 21st day, an equal volume of PBS was IP injected in the CONTROL and Sac/Val group.

All analyses were conducted after a 42-day period. The mice were anesthetized via intraperitoneal injection of sodium pentobarbital (50 mg/kg) and subsequently euthanized through bloodletting. Following euthanization, the heart was perfused and certain tissues were preserved in 4% paraformaldehyde for histological examination. The remaining tissues were promptly frozen for subsequent expression analysis.

Echocardiography

Transthoracic echocardiography was conducted utilizing a 30-MHz linear array ultrasound transducer (MS-400, VisualSonics Inc.), while administering 2% isoflurane. The papillary muscles were visualized through M-mode echocardiography using a short-axis view of the parasternal aspect of the heart. Left ventricular (LV) internal diameters were assessed during both diastole and systole, with LVEF and left ventricular fractional shortening (LVFS) being automatically computed. A tissue Doppler ultrasound was used to measure the E′ and A′ peaks inside the mitral valve orifice. The E′/A′ ratio was calculated as an indirect measure of diastolic function.

Histological studies

Following euthanasia of the rats, one-half of each heart ventricle was preserved in formalin and subsequently embedded in paraffin. Hematoxylin and eosin (H&E) as well as Masson's trichrome staining were utilized to evaluate myocardial morphology and inflammation in consecutive 4-mm-thick tissue sections. Semi-quantitative analysis of the stained tissues was conducted using Image-Pro plus software under a light microscope (Olympus, Japan).

Immunohistochemistry

Antigens were extracted from paraffin-embedded cardiac sections utilizing EDTA antigen retrieval buffer (pH 8.0) following deparaffinization and rehydration procedures. Subsequently, a 3% bovine serum albumin block was administered to rehydrated slides for a duration of 30 min, followed by the application of P62 rabbit antibody (#ab109012, Abcam, 1:400) overnight at 4 °C. The slides were then subjected to incubation with a secondary goat anti-rabbit antibody (#5220-0336, SeraCare Inc., USA, 1:200) in conjunction with avidin–biotin complex and horseradish peroxidase subsequent to PBS washing.

Cardiomyocyte size staining

To assess cardiomyocyte size, rehydrated slides were treated with 3% bovine serum albumin for 30 min and subsequently incubated overnight at 4 °C with FITC-conjugated wheat germ agglutinin (WGA) (#L4895, Sigma, USA). Cell nuclei were stained with 4′, 6-diamidino-2-phenylindole (DAPI, #C0065, Solarbio, Beijing), and fluorescent microscopes (Olympus, Tokyo) were employed for visualization of the stained sections.

Terminal deoxynucleotidyl transferase dUTP nick-end labeling (TUNEL) assay

Apoptotic cardiomyocytes in paraffin sections were identified using a TUNEL detection kit (#6432344001, Roche, USA) under a light microscope (Leica DM 4000 B; Leica, Wetzlar, Germany). Myocardial cytoskeleton colocalization with the anti-actin antibody (#23660-1-AP, Proteintech, Wuhan, 1:100) was observed. Slides were then treated with the goat anti-rabbit secondary antibody (FITC conjugate, #SA00003-2, Proteintech, Wuhan, 1:100). Four regions were randomly selected from each digitized image, and the number of apoptotic and healthy nuclei was quantified.

The apoptotic index was calculated as the number of TUNEL-positive nuclei/total number of nuclei [14, 19].

Evaluation of electron microscopy

The fixation process involved prefixing 1 mm^3 heart tissues for 4 h at 4 degrees Celsius with 2.5% glutaraldehyde immediately following tissue extraction from the left ventricle. Subsequently, the tissues were fixed at room temperature in 1% osmium tetroxide after rinsing with PBS. Dehydrated sections were then cut on an ultramicrotome (Leica UC 7, Leica) and stained with lead citrate and uranyl acetate. The ultrastructure of the autophagic vacuoles was examined using transient electron microscopy (TECNAI G2 20 TWIN, FEI), which is considered the gold standard for analyzing autophagy.

Detection of superoxide production

Dihydroethidium (DHE, #810253P, Sigma-Aldrich) staining was employed on frozen LV tissue (4 µm sections) to assess superoxide production. Fluorescence was detected using a fluorescent microscope (Olympus, Tokyo) with excitation and emission wavelengths of 488 nm and 568 nm, respectively.

Cell culture

It was described previously that Neonatal Sprague–Dawley rats (SD) were used to isolate ventricular myocytes (NRVMs) [19]. For Sac/Val pre-treatment following Dox-induced cardiomyocyte toxicity, NRVMs were pre-treated with 10 µM and 20 µM each of valsartan and LCZ696 for 12 h and then treated with 5 µM of DOX for 6 h [15]. Similar to animal experimental classification, an equal volume of PBS was incubated with NRVMs for 12 h in the CONTROL and Sac/Val group.

In-vitro reactive oxygen species (ROS) production measurement

Reactive oxygen species were quantified utilizing a 2′,7′-Dichlorofluorescin diacetate (DCF-DA) reagent (35,845, Sigma, USA) in this study. Various reagents were administered to neonatal rat ventricular myocytes (NRVMs) cultured in six-well plates for the duration of 18 h. Following 30-min incubation at 37 °C, the culture medium was replaced with serum-free medium containing 10 µm DCF-DA [19]. Fluorescent intensity was measured using excitation/emission wavelengths of 488/525 nm on a flow cytometer.

Cell viability detection

Cell viability was assessed using a Cell Counting Kit-8 (CCK-8, #CA1210, Solarbio, China) by incubating 10 mol CCK-8 solutions with NRVMs for one hour under standard incubation conditions. Viability was quantified by measuring the relative optical density of treated cells compared to untreated controls using a microplate reader (BioRad, USA).

Fluorescence-activated cell sorting (FACS) analysis

Fluorescein isothiocyanate (FITC)-conjugated annexin V and propidium iodide (PI) were utilized for the identification of apoptotic cells through the application of an apoptosis detection kit (KGA108, KeyGEN BioTECH, China) following the manufacturer's instructions [19]. NRVMs were resuspended in binding buffer and subsequently incubated with FITC-annexin V and PI at room temperature for approximately ten minutes. Fluorescence measurements were conducted using a flow cytometer (BD Biosciences) equipped with a FACS flow cytometer (BD Biosciences).

Real-time quantitative PCR (RT-qPCR)

The Trizol reagent (Invitrogen, Carlsbad, CA) was employed for total RNA extraction, followed by cDNA synthesis using the Prime Script RT reagent kit (Takara). Real-time qPCR was conducted using the StepOnePlus Real-Time PCR System (Applied Biosystems) in this study. Supplementary Table 1 provides a comprehensive list of primer sequences utilized for assessing relative gene expression levels with GAPDH serving as the reference gene.

Western blot analysis

Radiation immunoprecipitation (RIPA) buffer (#R0010, Solarbio, Beijing) was utilized for the homogenization and lysis of heart tissue or NRVMs prior to electrotransfer onto PVDF membranes (Millipore, USA). Subsequently, the

membranes were blocked in TBST buffer and incubated with primary antibodies (Supplementary Table 2) overnight at −4 °C. Immunoreactive bands were then detected by incubating with a secondary antibody (Boster, Wuhan, China) conjugated with horseradish peroxidase (HRP) and visualized using a chemiluminescence system (ECL, GE Healthcare Bio-Sciences).

Statistical analysis

Analysis of Variance (ANOVA) was employed for the examination of data involving multiple comparisons, with post hoc tests such as the Least Significant Difference (LSD) test assuming equal variances, and Dunnett's T3 test in cases where equal variances were not assumed. The study utilized Graphpad Prism 8.0 software (GraphPad Software Inc., CA, USA) and SPSS version 26 (IBM, Armonk, New York) for statistical analysis. A significance level of $P < 0.05$ was deemed statistically significant.

Results

Sac/Val treatment inhibited myocardium inflammation

In comparison to the control groups, mice with DOX-induced cardiotoxicity demonstrated inflammatory cell infiltration in the myocardium as observed through H&E staining (Fig. 1A). Mononuclear macrophages were the predominant cell type infiltrating the myocardial interstitium. Treatment with Sac/Val was shown to decrease this inflammatory infiltration in the myocardium. The mRNA levels of inflammatory cytokines, including IL-1β, IFN-γ, TNF-α, and MCP-1, were significantly elevated in the myocardium of mice with DOX-induced cardiotoxicity in the DOX groups compared to the CONTROL group ($P < 0.01$ for all comparisons, Fig. 1B–E). The mRNA levels of the aforementioned inflammatory cytokines were notably reduced in the Sac/Val + DOX group compared to the DOX group ($P < 0.05$ for all comparisons, as shown in Fig. 1B–E). Additionally, western blot analysis revealed an increase in the protein expression of NLRP3 and Caspase-1 in the myocardium of mice with DOX-induced cardiotoxicity compared to the CONTROL group, with Sac/Val treatment partially restoring the protein expression of NLRP3 and Caspase-1 in the cardiotoxic hearts (Fig. 2A–D). These findings suggested that Sac/Val treatment could ameliorate DOX-induced cardiotoxicity by the deregulation of myocardial inflammation.

Sac/Val treatment inhibited cardiac fibrosis

In comparison to the control groups, mice with DOX-induced cardiotoxicity displayed notable collagen matrix deposition in the myocardium as evidenced by Masson's trichrome staining. Subsequent treatment with Sacubitril/Valsartan (Sac/Val) was found to mitigate this myocardial fibrosis (see Fig. 3A, B). Additionally, western blot analysis revealed that the protein expression of Collagen I in the myocardium of DOX-induced cardiotoxic mice was elevated compared to the control groups, with Sac/Val treatment partially restoring Collagen I protein expression in the cardiotoxic hearts (see Fig. 3C, D). The mRNA levels of fibrotic factors, including α-SMA, Collagen I, and Collagen III, were found to be significantly elevated in the myocardium of mice with DOX-induced cardiotoxicity in the DOX groups compared to the CONTROL group ($P < 0.01$ for all comparisons, Fig. 2E–G). Conversely, the mRNA levels of these fibrotic factors were significantly reduced in the Sac/Val + DOX group compared to the DOX group ($P < 0.05$ for all comparisons, Fig. 3E–G). These results indicated that Sac/Val treatment may mitigate DOX-induced cardiotoxicity by suppressing cardiac fibrosis.

Sac/Val treatment inhibited cardiomyocyte hypertrophy

In comparison to the control groups, mice with DOX-induced cardiotoxicity exhibited a significantly larger cardiomyocyte size in the myocardium as indicated by WGA staining (Fig. 4A, B) and an increased ratio of heart weight to body weight (Fig. 4C). Treatment with Sac/Val was found to mitigate this cardiomyocyte hypertrophy and heart weight-to-body weight ratio (Fig. 4A–C). The mRNA levels of cardiac fetal reactivation genes, including atrial natriuretic peptide (ANP), brain natriuretic peptide (BNP), and β-myosin heavy chain (MHC), were found to be significantly elevated in the myocardium of mice with Dox-induced cardiotoxicity in the DOX groups compared to the CONTROL group ($P < 0.05$ for all comparisons, Fig. 4D–F). Conversely, the mRNA levels of these cardiomyocyte hypertrophy factors were significantly reduced in the Sac/Val + DOX group compared to the DOX group ($P < 0.05$ for all comparisons, Fig. 4D–F). These findings suggested that Sac/Val treatment could ameliorate Dox-induced cardiotoxicity by the inhibiting myocardial hypertrophy.

Sac/Val treatment improved myocardial apoptosis

In comparison to the control groups, the myocardium of mice with DOX-induced cardiotoxicity exhibited increased protein expression of pro-apoptotic bax, as well as a notable increase in cleaved caspase-3 and cleaved caspase-9, and

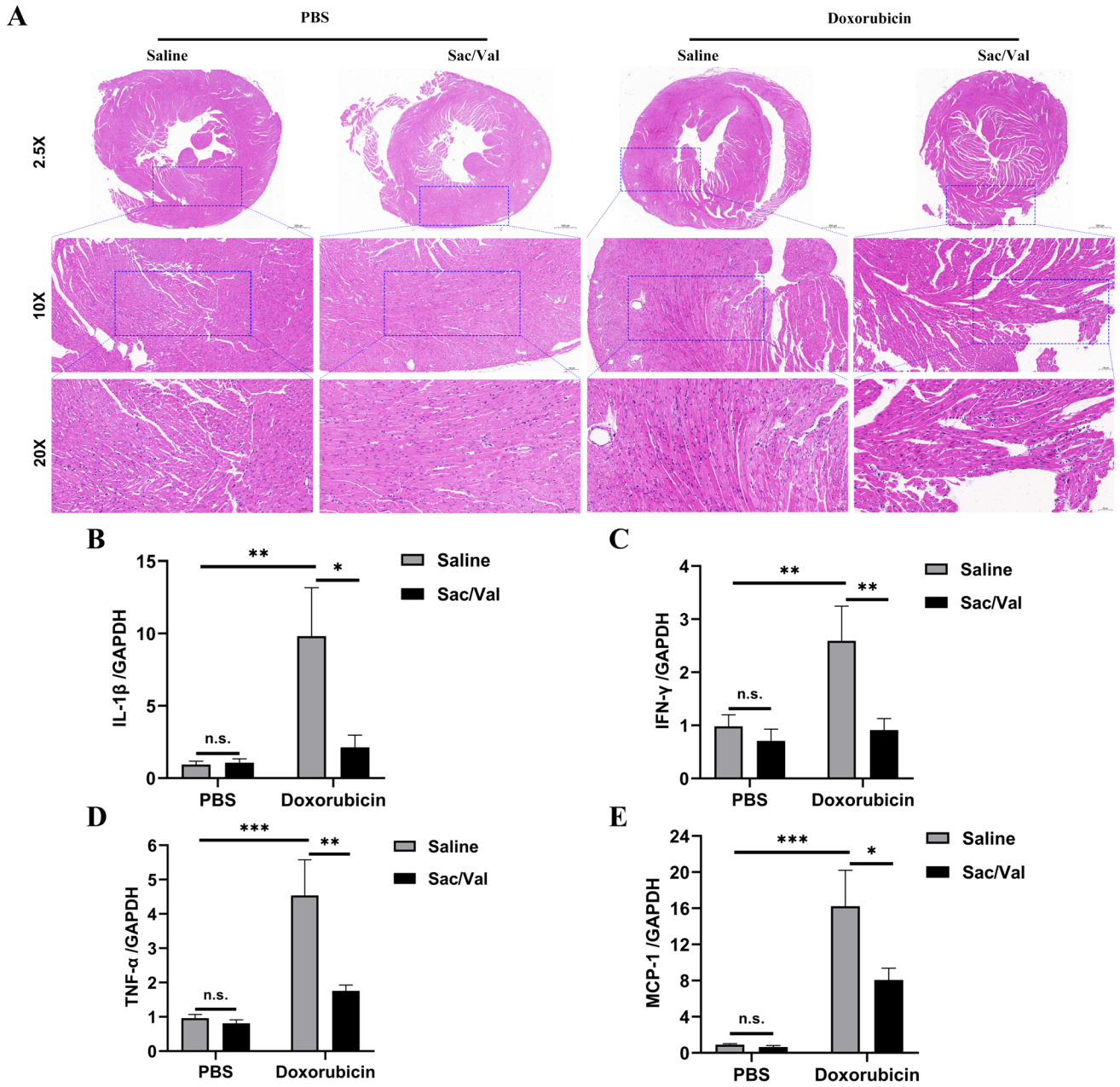

Fig. 1 Inflammatory cell infiltration in the myocardium. **A** Representative images of inflammatory cell infiltration into the myocardium according to H&E staining from the different groups ($n=5$ per group, magnification = 200×). **B**–**E** The mRNA expression of inflammatory cytokines including IL-1β, IFN-γ, TNF-α, and MCP-1 was determined by quantitative RT-PCR in the myocardium from the different groups ($n=6$ per group). The values were normalized to the housekeeping gene GAPDH. The data are represented as the means ± SE; * $P<0.05$, ** $P<0.01$, *** $P<0.001$

a significant decrease in anti-apoptotic Bcl-2 (Fig. 5A–F). Subsequent treatment with Sac/Val partially reversed the alterations in expression of apoptosis-related proteins in the myocardium of DOX-induced cardiotoxicity mice (Fig. 5A–F). DOX-induced cardiotoxicity mice showed a higher proportion of apoptosis in cardiac myocytes according to TUNEL staining as compared to that in controls, which was partly reversed by Sac/Val treatment (Fig. 6A, B). These findings suggested that Sac/Val treatment improved myocardial apoptosis in DOX-induced cardiotoxicity mice.

Sac/Val treatment promoted myocardial autophagy

To determine the effects of Sac/Val treatment on DOX-induced myocardial lessened autophagy, we performed immune-histochemical analysis of P62 protein to assess

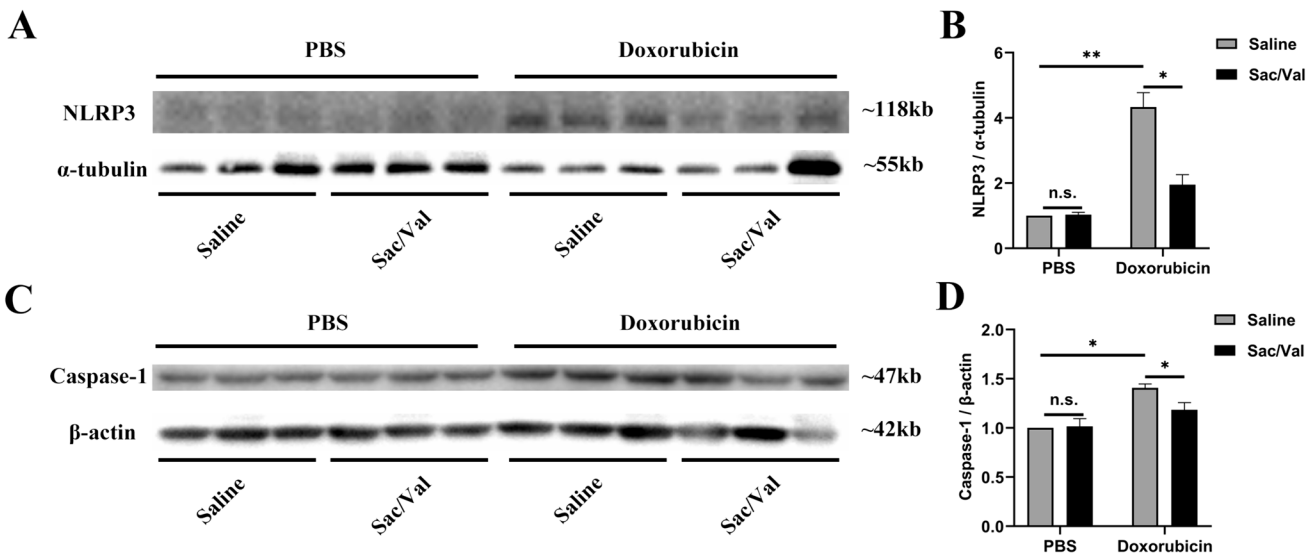

Fig. 2 Myocardium inflammation DOX-induced cardiotoxicity mice. **A** Representative western blot image of NLRP3 in the myocardium from the different groups. The α-tubulin was used as a loading control. **B** Corresponding densitometric analysis of blots in A ($n=6$ per group). **C** Representative western blot image of Caspase-1 in the myocardium from the different groups. The β-actin was used as a loading control. **D** Corresponding densitometric analysis of blots in **C** ($n=6$ per group). The data are represented as the means ± SE; * $P<0.05$, ** $P<0.01$

cardiomyocyte autophagy. DOX-induced cardiotoxicity mice showed a higher proportion of P62 positive cells as shown by immunohistochemistry as compared to that in controls, which was ameliorated by Sac/Val treatment (Fig. 7A, B). Western blotting showed that compared to the control arms, the autophagy-related protein expression of P62 increased significantly, of ULK1 and LC3-II decreased obviously in the myocardium of DOX-induced cardiotoxicity mice, which was also reversed by Sac/Val treatment (Fig. 7C–G).

The ultrastructural morphologies of the hearts were observed by transmission electron microscopy. The DOX-induced cardiotoxicity mice showed a lower proportion of autophagic-like vesicles as compared to that in controls, which was reversed by Sac/Val treatment (Supplementary Fig. 1A, B). These findings suggested that Sac/Val treatment promoted myocardial lessened autophagy in DOX-induced cardiotoxicity mice.

Sac/Val treatment improved systolic and diastolic function

Echocardiographic analysis of cardiac function in mice treated with Doxorubicin revealed a reduction in left ventricular ejection fraction (LVEF) and left ventricular fractional shortening (LVFS), indicating a deterioration in cardiac systolic function compared to control mice. This impairment was mitigated by treatment with Sacubitril/Valsartan (Sac/Val), as shown in Fig. 8A, B. Additionally, a significant decrease in the ratio of E versus A and E′ versus A′, indicative of worsened cardiac diastolic function, was observed in DOX-treated mice. This diastolic dysfunction was reversed by Sac/Val treatment, as illustrated in Fig. 8C–F.

Changes in AMPKα–mTORC1 signaling pathway

Mice with DOX-induced cardiotoxicity demonstrated increased protein expression of p-AMPKα in heart homogenates compared to controls, a change that was reversed by Sac/Val treatment (Fig. 9A, B). Additionally, these mice exhibited decreased protein expression levels of p-mTOR(Ser2448), Raptor, p-S6K1(Thr389), and p-4EBP1(Thr37/46) in heart homogenates compared to controls, which were also reversed by Sac/Val treatment (Fig. 9C–G). Besides, DOX-induced cardiotoxicity mice exhibited an increased oxidative stress level in myocardium according to DHE staining as compared to that in controls, which was partly reversed by Sac/Val treatment (Supplementary Fig. 2A, B).

Sac/Val treatment defended against Dox-induced apoptosis and autophagy inhibition in primary cardiomyocytes

In comparison to the control group, the viability of cardiomyocytes exhibited a significant decrease following stimulation with DOX, a decrease that was partially ameliorated by treatment with Sac/Val (Fig. 10A). Similarly, the apoptosis

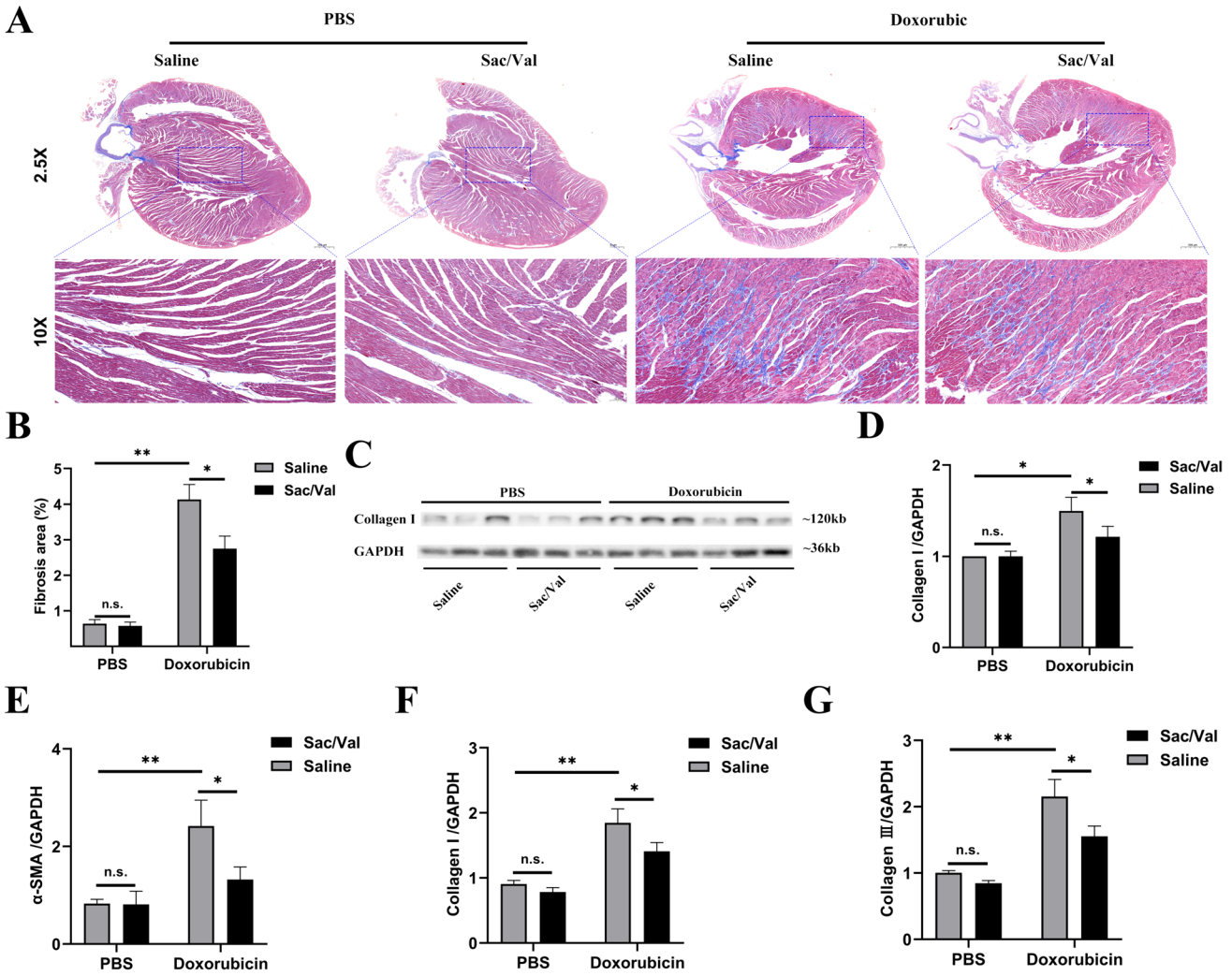

Fig. 3 Cardiac fibrosis in DOX-induced cardiotoxicity mice. **A** Representative images of collagen matrix deposition in the myocardium according to Masson's trichrome staining from the different groups (magnification = 50×). **B** Corresponding statistic analysis of cardiac fibrosis in **A** ($n = 5$ per group). **C** Representative western blot image of Collagen I in the myocardium from the different groups. The GAPDH was used as a loading control. **D** Corresponding densitometric analysis of blots in **C** ($n = 6$ per group). **E–G** The mRNA expression of fibrotic factors such as α-SMA, Collagen I, and Collagen III, was determined by quantitative RT-PCR in the myocardium from the different groups ($n = 4$ per group). The values were normalized to the housekeeping gene GAPDH. The data are represented as the means ± SE; * $P < 0.05$, ** $P < 0.01$

level of primary cardiomyocytes significantly increased after exposure to DOX, but was partially mitigated by Sac/Val treatment (Fig. 10B, C). Additionally, the protein expression levels of pro-apoptotic cleaved Caspase-3 increased significantly, while the ratio of Bcl-2/Bax decreased in primary cardiomyocytes following DOX stimulation, with partial restoration observed after treatment with Sac/Val (Fig. 10D, F, G). Sac/Val treatment defended against the DOX-induced expression of apoptosis-related proteins in primary cardiomyocytes. The protein expression levels of P62 significantly increased and LC3-II significantly decreased in primary cardiomyocytes after DOX stimulation, compared to controls. This effect was partially reversed by Sac/Val treatment, as shown in Fig. 10E, H, I. These findings indicate that Sac/Val treatment may partially restore the DOX-induced apoptosis and autophagy inhibition in primary cardiomyocytes.

Sac/Val treatment defended against Dox-induced apoptosis and autophagy inhibition in primary cardiomyocytes via regulating the AMPKα–mTORC1signaling pathway

As illustrated in Fig. 11A, B, the levels of ROS in primary cardiomyocytes significantly increased following 24 h of DOX stimulation compared to controls, a change that was

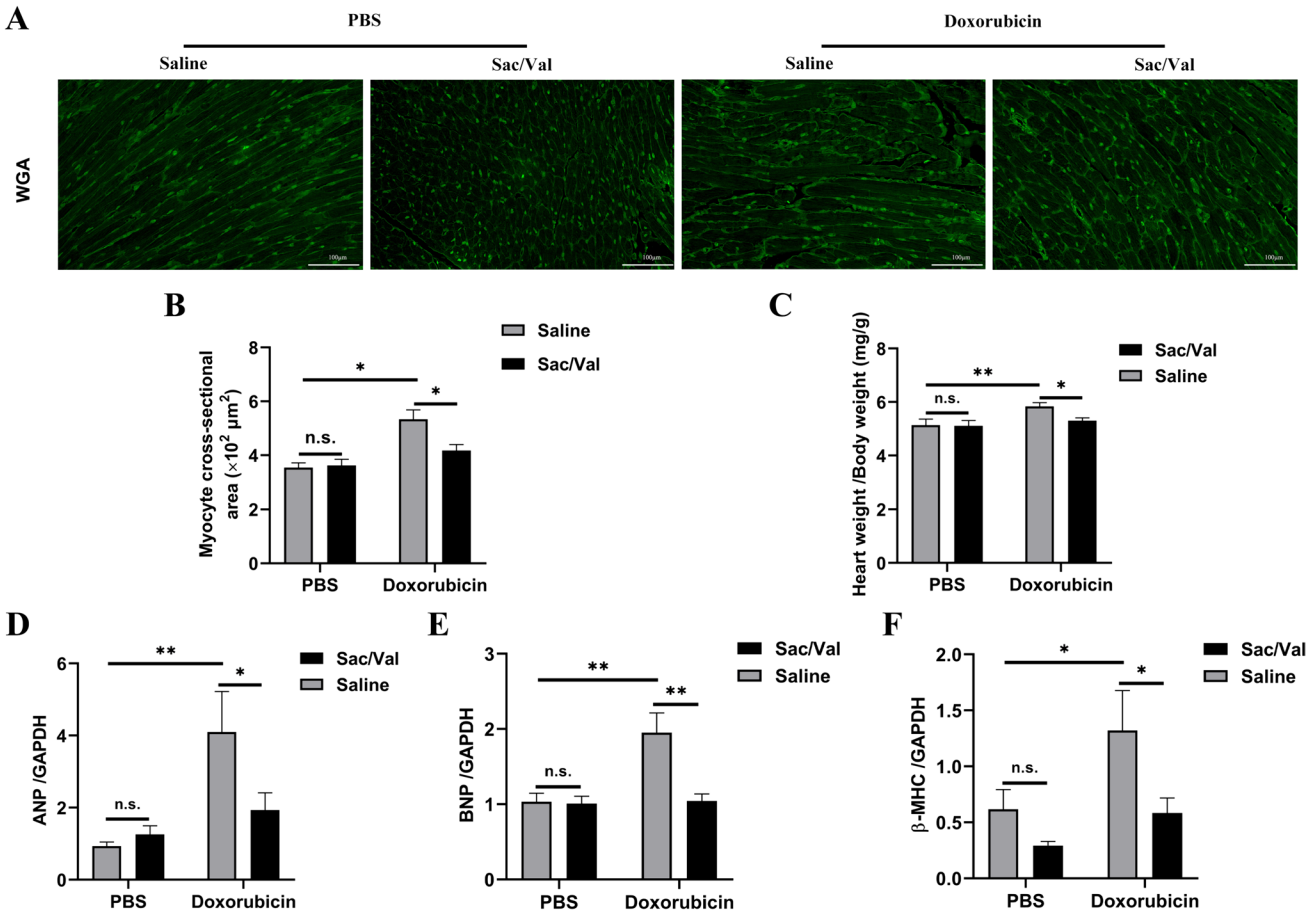

Fig. 4 Cardiomyocyte hypertrophy in DOX-induced cardiotoxicity mice. **A** Representative staining images of wheat germ agglutinin (WGA) in mice hearts from the different groups. **B** Corresponding statistic analysis of cardiomyocyte size used WGA staining in **A** ($n=5$ per group). **C** The ratio of mouse heart weight versus body weight from the different groups ($n=8$ per group). **D**–**F** The mRNA expression of ANP, BNP, and β-MHC detected by RT-qPCR in the myocardium from the different groups ($n=6$ per group). The values were normalized to the housekeeping gene GAPDH. The data are represented as the means ± SE; * $P<0.05$, ** $P<0.01$

mitigated by prior incubation with Sac/Val. Additionally, DOX stimulation resulted in an elevated protein expression of p-AMPKα in primary cardiomyocytes, an effect that was partially attenuated by treatment with Sac/Val (Fig. 11C, D). In comparison to the control group, the protein expression levels of p-mTOR (Ser2448), Raptor, p-S6K1 (Thr389), and p-4EBP1 (Thr37/46) were notably reduced following DOX stimulation in primary cardiomyocytes, with partial restoration observed after Sac/Val treatment (Fig. 11E–I). These findings indicated that the AMPKα signaling pathway was increased, the mTORC1 signaling pathway was decreased under the context of DOX-induced cardiotoxicity, that were partially attenuated by treatment with Sac/Val. These results offer a molecular rationale for the anti-apoptotic and de-autophagy effects by Sac/Val via regulation of the AMPKα–mTORC1 signaling pathway in the context of DOX-induced cardiotoxicity.

Discussion

As advancements in cancer treatment lead to increased survival rates, the long-term cardiovascular side effects of chemotherapy, particularly anthracyclines used in the treatment of various cancers such as breast cancer, have become a significant concern due to their dose-dependent cardiotoxicity [1, 5]. Chemotherapy-induced cardiotoxicity was the second leading cause of mortality among cancer patients [1, 5]. This adverse outcome encompassed many cardiovascular problems, such as heart failure. The manifestation of these cardiotoxic effects could vary in timing, from early to late after exposure to specific chemotherapy agents. The incidence and impact of cardiotoxicity differed from one chemotherapeutic agent to another, depending on the intensity and mechanism of action of the chemotherapy [1, 5].

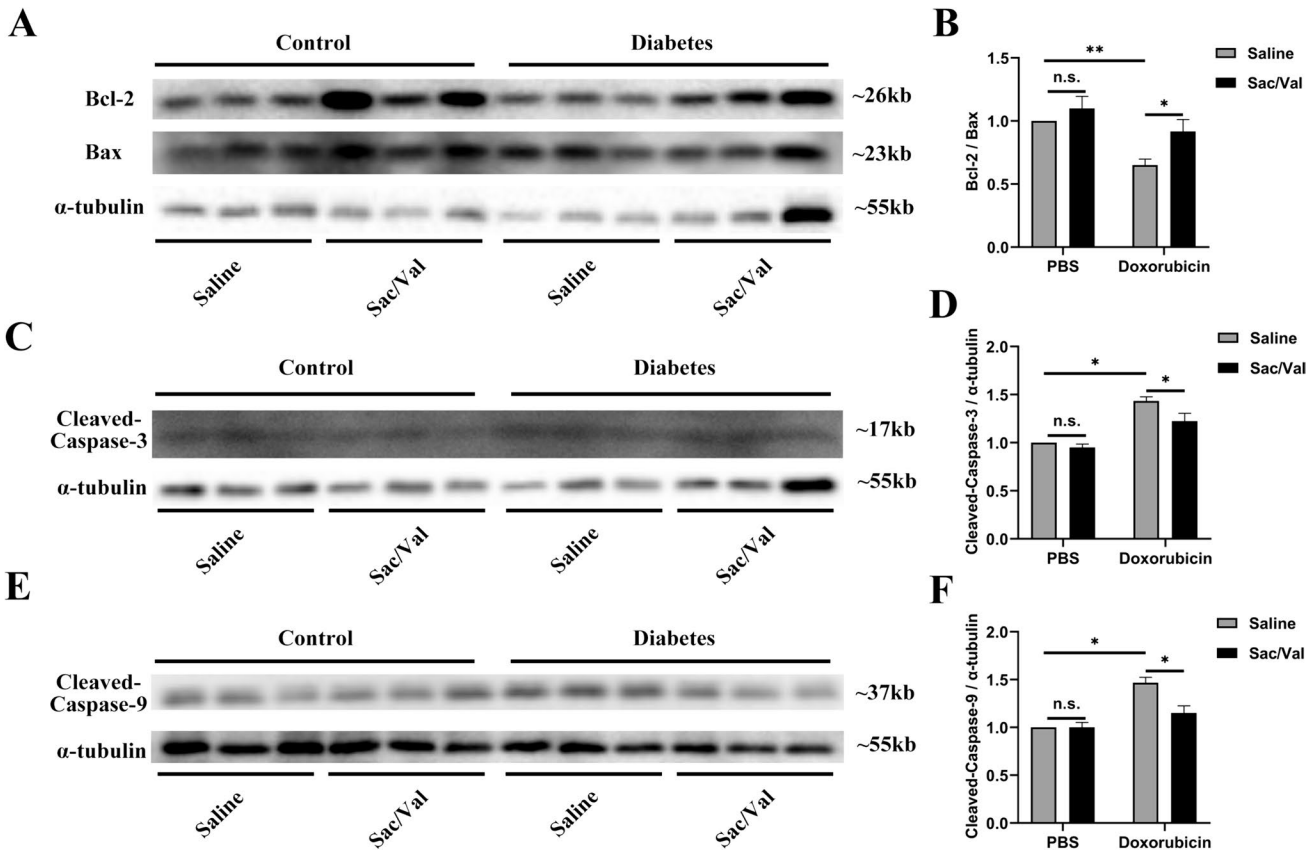

Fig. 5 The apoptosis-related proteins in DOX-induced cardiotoxicity mice. **A** Representative western blot image of Bax and Bcl-2 in the myocardium from the different groups. **B** Corresponding densitometric analysis of blots in **A** ($n=6$ per group). **C** Representative western blot image of cleaved caspase-3 in the myocardium from the different groups. **D** Corresponding densitometric analysis of blots in **C** ($n=6$ per group). **E** Representative western blot image of cleaved caspase-9 in the myocardium from the different groups. **F** Corresponding densitometric analysis of blots in **E** ($n=6$ per group). The α-tubulin was used as a loading control. The data are represented as the means ± SE; * $P<0.05$, ** $P<0.01$

To effectively address the development of CTRCD, it is imperative to gain a comprehensive understanding of the underlying mechanisms. Among the various factors contributing to anthracycline-induced cardiotoxicity, lipid peroxidation of the cell membrane emerged as a primary cause. The generation of ROS through iron-dependent pathways is identified as the predominant source of anthracycline-induced cardiotoxicity [5]. Some previous findings have shown that ferroptosis played a key role in progression of DOX-induced cardiotoxicity. It has been demonstrated that heme oxygenase one-dependent heme degradation and free iron overload promoted ferroptosis and anthracycline-induced cardiotoxicity [20]. Furthermore, doxorubicin has been shown to suppress mGPX4 expression thereby inducing excessive lipid peroxidation in mitochondria and might consequently lead to mitochondria-dependent ferroptosis. The overexpression of mGPX4 or iron chelation targeting mitochondrial iron content significantly prevented DOX-induced ferroptosis [21].

Doxorubicin exerted its cytotoxic effect by intercalating DNA. When doxorubicin bound to Top2β and DNA, mitochondrial dysfunction was triggered by the suppression of peroxisome proliferator-activated receptor (PPAR), resulting in an activation of altered P53 tumor suppressor pathway, β-adrenergic signaling, impaired calcium handling, and increased apoptosis [22]. Animal studies with cardiomyocyte-specific deletion of Top2β protected mice from doxorubicin-induced cardiotoxicity partially due to reduced DNA double-strand breaks and transcriptome changes that were responsible for defective mitochondrial biogenesis and ROS formation [5, 23]. Willis et al. [24] demonstrated subacute anthracycline-induced decrease in cardiac mass in both mice and humans. Muscle-specific ubiquitin ligase muscle ring finger-1 (MuRF1) $^{-/-}$ mice were protected from DOX-induced cardiac atrophy and exhibited no reduction in contractile function.

A 22-year-old male patient with acute myeloid leukemia who had developed to CTRCD early detected by an asymptomatic decrease in LVEF and global longitudinal strain (GLS), completed full-process chemotherapy regime and hematopoietic stem cell transplantation plan after

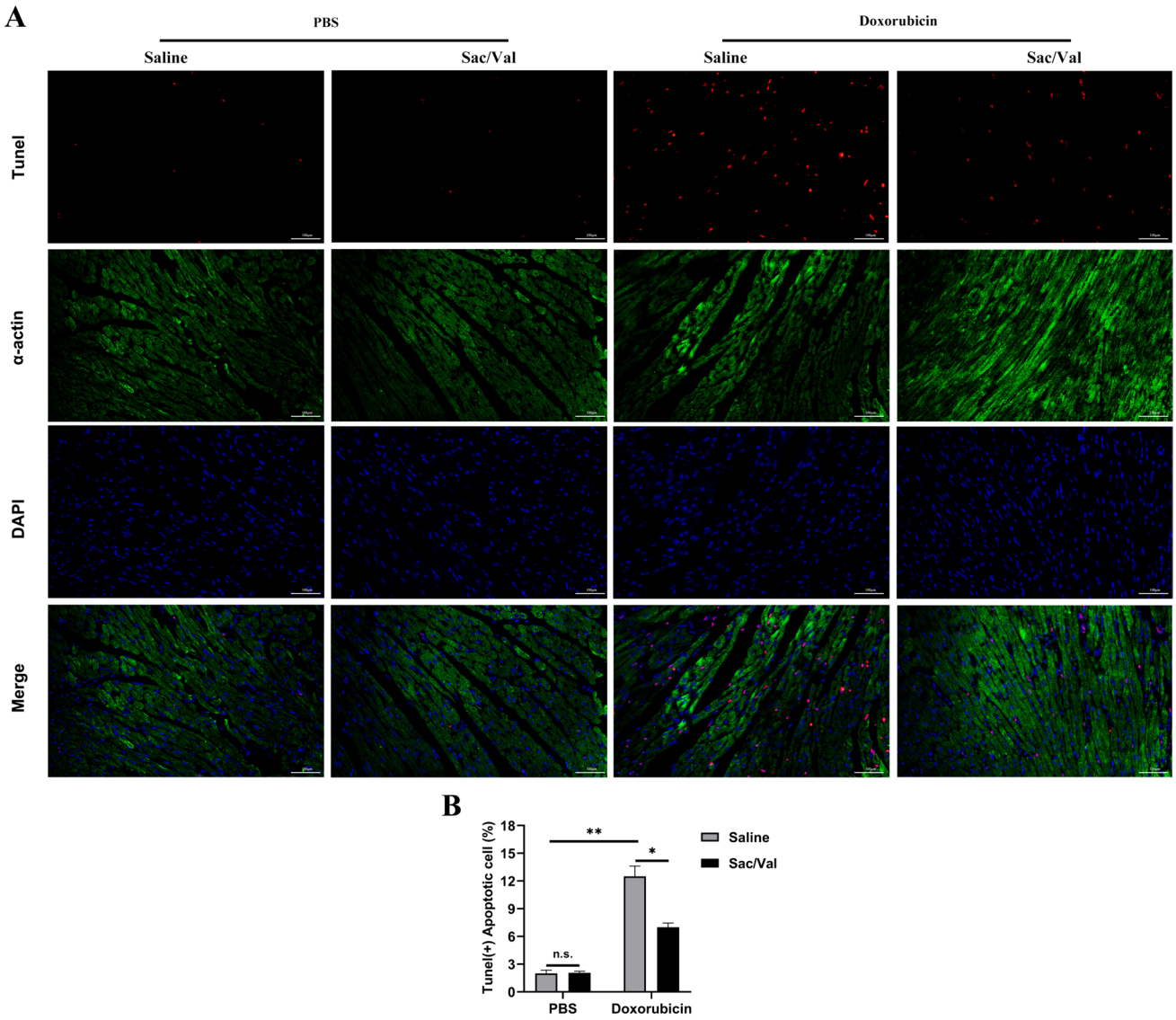

Fig. 6 Myocardial apoptosis detected by the TUNEL staining. **A** Representative images of TUNEL staining in the myocardium from the different groups. The α-actin staining was used for colocalization of cardiomyocytes and DAPI was used for nuclear staining. **B** Corresponding statistic analysis of cardiomyocyte apoptosis in **A** ($n=5$ per group). The data are represented as the means ± SE; $^{*}P<0.05$, $^{**}P<0.01$

receiving Sac/Val [25]. One nearest case series revealed a considerable improvement in LVEF in six out of eight patients who had chemotherapy-induced cardiomyopathy after receiving Sac/Val treatment [26]. A 68-year-old female patient with a pleural epithelioid angiosarcoma developed CTRCD following DOX treatment. Despite a continuous application of the cardioprotective medical treatment regimen, no improvement of LVEF was detected in a 4-month follow-up. Then after omitting ramipril and implementing low-dose Sac/Val, it was observed that a decrease in serum biomarkers within 3 months as well as a significant improvement of LVEF within 6 month [27]. The above results indicated that Sac/Val is a promising option for the management of CTRCD even in those with a delayed diagnosis.

In this study, we examined the prophylactic properties of Sac/Val in mitigating DOX-induced cardiotoxicity and elucidated the potential underlying mechanisms. Our findings demonstrated that pre-treatment with Sac/Val could mitigate DOX-induced apoptosis myocardial apoptosis, while promoting autophagy assessed by western blots and transmission electron microscope and improving systolic function evaluated by M model Teich's method in mice or primary cardiomyocytes through modulation of the AMPKα–mTORC1 pathway. These results offered a molecular rationale for the improvement of

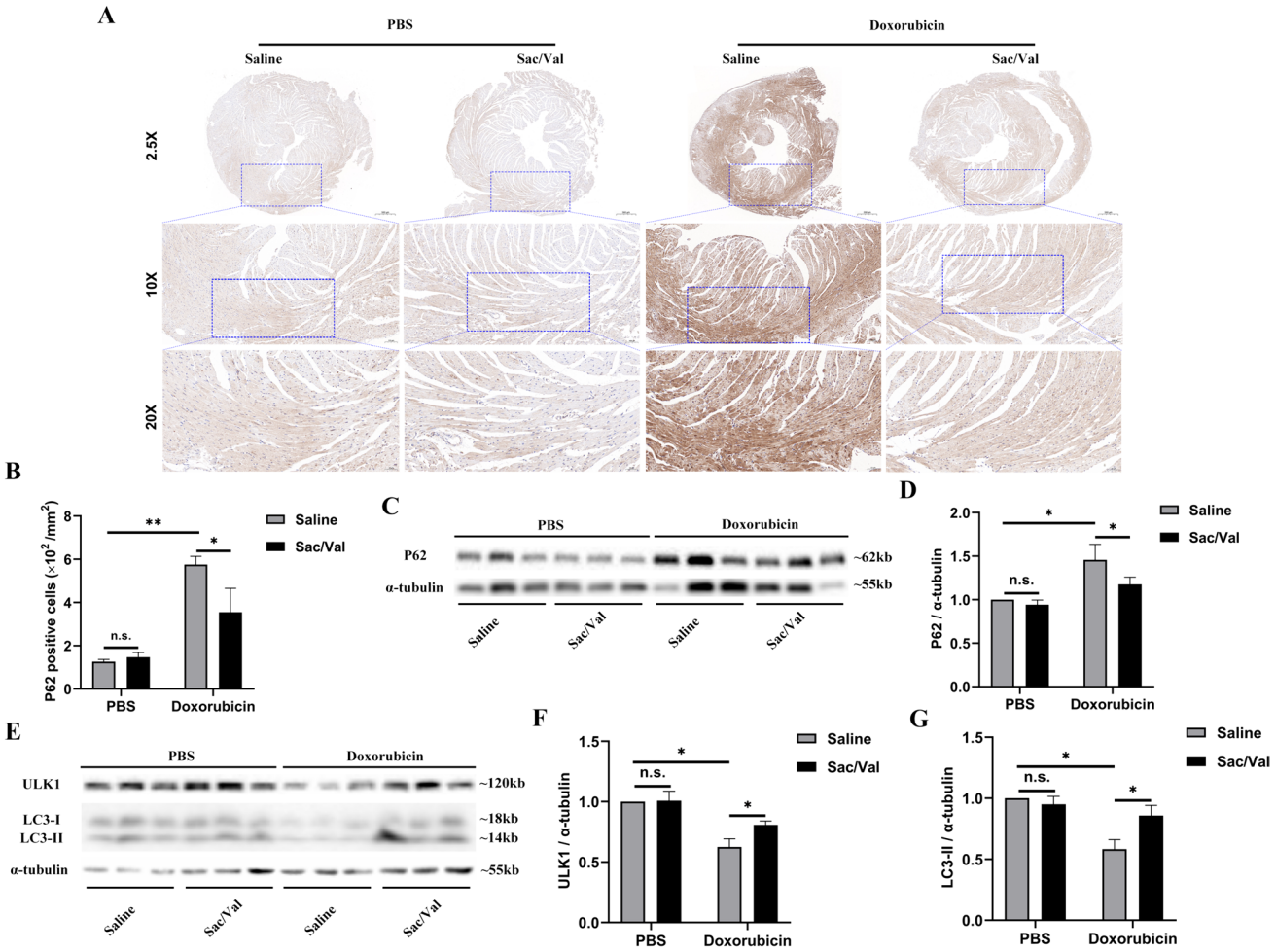

Fig. 7 Sac/Val treatment promoted myocardial autophagy in DOX-induced cardiotoxicity mice. **A** Immunohistochemical analysis of autophagy substrates P62 protein in mice hearts from the different groups (magnification = 200×). **B** Corresponding statistic analysis of P62 in **A** ($n = 5$ per group). **C** Representative western blot image of P62 in the myocardium in each group. The α-tubulin was used as a loading control. **D** Corresponding densitometric analysis of blots in **C** ($n = 6$ per group). **E** Heart homogenates were analyzed by western blot using an antibody against LC3 II/I and ULK1 proteins. The α-tubulin was used as a loading control. **F**, **G** Corresponding densitometric analysis of blots in **E** ($n = 6$ per group). The data are represented as the means ± SE; $^{*}P < 0.05$, $^{**}P < 0.01$

DOX-induced cardiotoxicity by Sac/Val via regulation of the AMPKα–mTORC1 signaling pathway.

In the context of cardio-oncology, treatment-induced cardiotoxicity posed a significant risk to patient health. Sac/Val regimen was recommended for managing this complication. A retrospective case study documented successful outcomes with Sac/Val treatment in two individuals with anthracycline-related cardiomyopathy and HFrEF who had previously shown poor responses to conventional evidence-based medications [28]. Both patients experienced improvements in heart failure symptoms, normalization of NT-proBNP levels, and avoided rehospitalization for their condition [28]. Canale et al. [29] presented a case series involving four patients diagnosed with CTRCD and severe HFrEF. The patients received Sac/Val treatment while wearing an automatic defibrillator until their cardiac function normalized. A subsequent study conducted by researchers in six Spanish hospitals with specialized cardio-oncology clinics followed up on 67 cancer survivors, the majority of whom had received anthracycline-based chemotherapy [30]. Among patients with HFrEF, Sac/Val therapy was found to be well tolerated and associated with improvements in NT-proBNP levels, NYHA functional class, and echocardiographic findings [30]. Renato et al. [31] reported that anthracycline cardiomyopathy was treated with Sac/Val in two clinical cases, where symptoms and echocardiographic parameters improved in response to the treatment. Ana et al. [32] evaluated ten consecutive patients suffering from cardiotoxicity-related HFrEF, they were evaluated by comprehensive multiparametric cardiac magnetic resonance (CMR) for the therapeutic effect of Sac/Val. When Sac/Val was administered, LV volumes were markedly reduced and

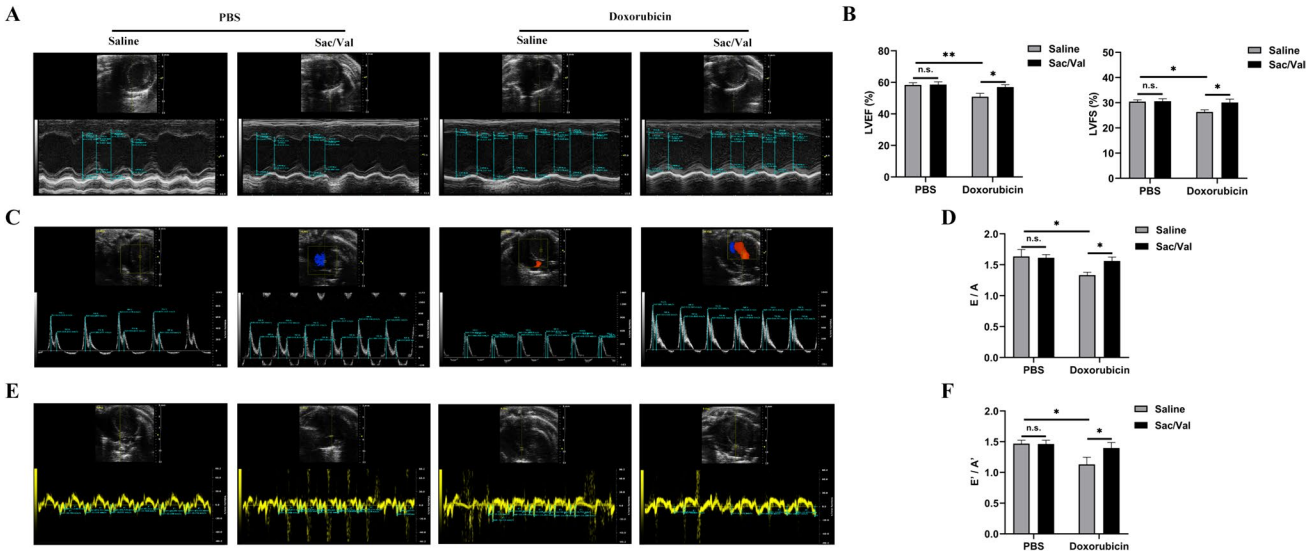

Fig. 8 Cardiac function measured by echocardiography. **A** Representative images by M-mode echocardiography in mice hearts from the different groups. **B** Echocardiography analysis showing cardiac systolic dysfunction assessed by LVEF and LVFS ($n=5$ per group). **C** The ratio of the peak mitral valve blood velocity during early diastolic period **E** versus peak mitral valve blood velocity during late diastolic period **A**. **D** The diastolic dysfunction assessed by the ratio of E versus A ($n=5$ per group). **E** Representative images by pulsed wave Doppler echocardiography in mice hearts from the different groups. **F** The diastolic dysfunction assessed by ratio of diastolic mitral annulus velocities (E′ versus A′) **E** ($n=5$ per group). The data are represented as the means ± SE; $^{*}P<0.05$, $^{**}P<0.01$

LVEF was significantly improved. NYHA functional class also improved in association with a marked decrease in NT-proBNP concentration [32]. The LV dysfunction within CTRCD was partly restorable, but this strongly depended on timely treatment with Sac/Val [32]. After failing to respond to conventional evidence-based drug therapy, Sac/Val was introduced to 28 patients with breast cancer and refractory cardiotoxicity-related HFrEF [33]. The NYHA cardiac function grade, six-minute walking distance, LVEF, LV diastolic function, LV end-diastolic diameter, and mitral regurgitation assessment significantly improved after captopril or valsartan was replaced with ARNI. While several small observational studies have found that Sac/Val improves cardiac structure and function in CTRCD patients, large-scale prospective clinical trials are needed to confirm these findings.

Studies on the efficacy of Sac/Val in mitigating doxorubicin-induced cardiotoxicity in animal experimental models are limited. Following administration of doxorubicin, mice exhibited impaired heart function, abnormal mitochondrial structure, and compromised respiratory function, all of which were significantly improved with Sac/Val treatment [11]. Additionally, it is suggested that sacubitril/valsartan may enhance dynamin-related protein 1 (Drp1)-mediated mitochondrial dysfunction caused by doxorubicin [11]. In a preclinical model of prophylactic treatment, Sac/Val demonstrated efficacy in mitigating oxidative stress damage, inflammation, and apoptosis associated with DOX-induced heart failure and arrhythmia [12]. Furthermore, compared to doxorubicin alone, Sac/Val attenuated matrix metalloproteinase (MMP) activity in rats, thereby safeguarding against doxorubicin-induced cardiac systolic dysfunction and left ventricular remodeling [13]. Rats administered with Sac/Val exhibited significant amelioration of doxorubicin-induced cardiac dysfunction through the downregulation of endoplasmic reticulum stress and apoptosis-related proteins [14]. The mitigation of cardiotoxicity induced by doxorubicin in rat hearts and H9C2 cardiomyocytes was achieved through the reduction of oxidative stress by Sac/Val [15]. These findings suggested that the cardiotoxic effects of doxorubicin might have been attenuated by the anti-inflammatory, anti-apoptotic, and antioxidant properties of Sac/Val.

Based on the data presented, the cardiotoxic effects induced by DOX might have been mitigated by the anti-inflammatory, anti-apoptotic, and antioxidant properties [34]. Activation of autophagy at a moderate level might support cellular energy and nutrient provision, thereby safeguarding cardiomyocytes [34]. Notably, our findings demonstrated for the first time that Sac/Val treatment could ameliorate autophagy suppression in mice with DOX-induced cardiotoxicity.

AMPK, a heterotrimeric enzyme, played a crucial role in regulating cardiac energy homeostasis [35]. The serine/threonine-specific protein kinase, mTOR, consists of two distinct multi-complexes, mTORC1, which is involved in regulating cardiac autophagy in response to oxidative stress [19]. The deficiency of soluble epoxide hydrolase has been shown to reduce myocardial lipid accumulation by enhancing AMPK–mTORC-mediated autophagy [35].

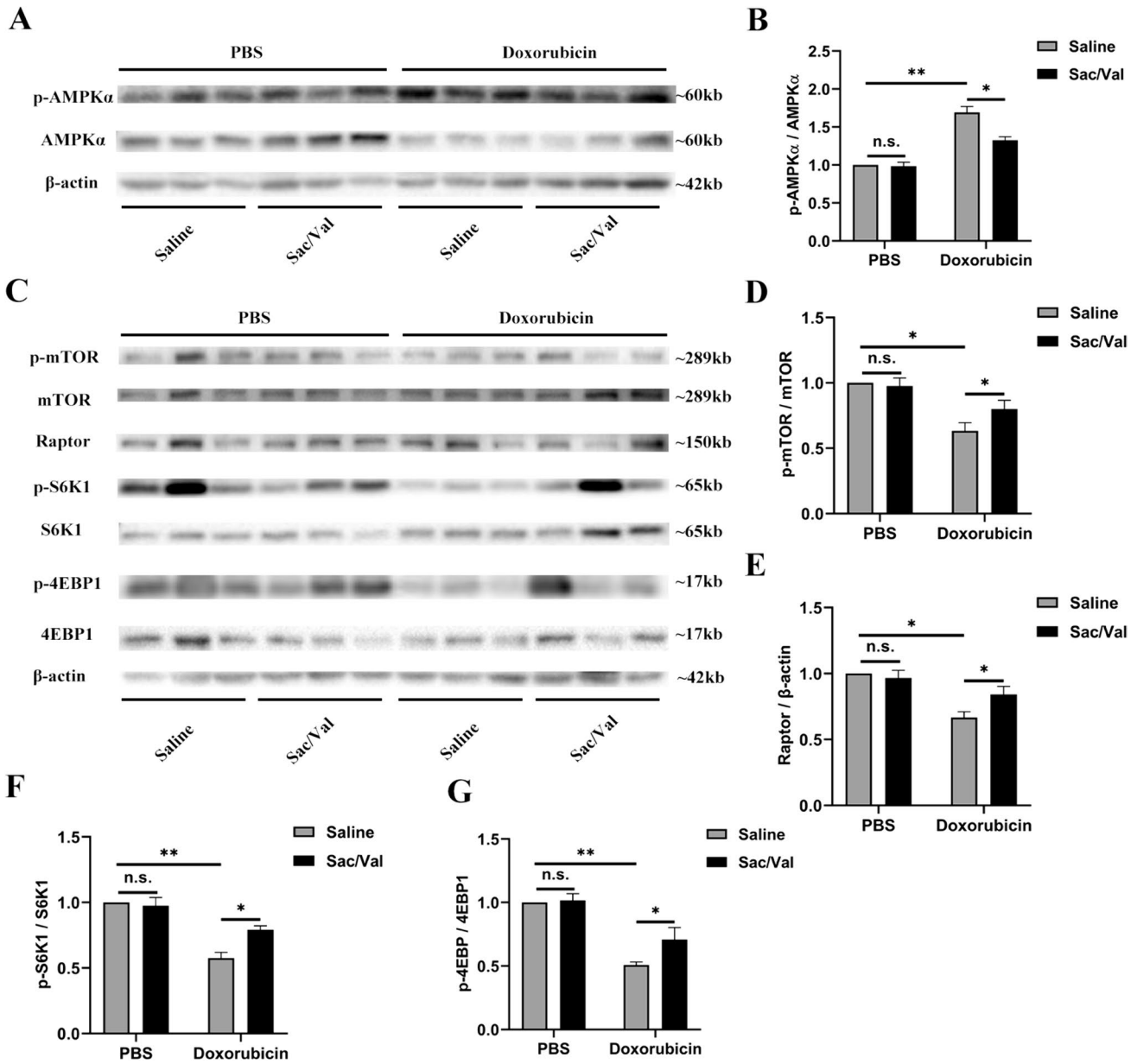

Fig. 9 Changes in AMPKα–mTORC1 signaling pathway in DOX-induced cardiotoxicity mice. **A** Representative western blot analyses of p-AMPKα and AMPKα in mice heart homogenates from the different groups. **B** Corresponding densitometric analysis of blots in **A** ($n=6$ per group). **C** Representative western blot analyses of p-mTOR (Ser2448) and mTOR, Raptor, p-S6K1 (Thr389) and S6K1, and p-4EBP1 (Thr37/46) and 4EBP1 in mice heart homogenates from the different groups. **D**–**G** Corresponding densitometric analysis of blots in **C** ($n=6$ per group). The β-actin was used as a loading control. The data are represented as the means ± SE; $^{*}P<0.05$, $^{**}P<0.01$

Our study demonstrated that Sac/Val exhibited cardioprotective effects against DOX-induced cardiotoxicity through its anti-apoptotic and de-autophagy properties, mediated by the regulation of the AMPKα–mTORC1 signaling pathway. Our work contributed to the molecular rationale for the improvement of DOX-induced cardiotoxicity by Sac/Val, therefore enabling cancer patients to continue crucial oncological therapies. Further basic and clinical research is necessary to thoroughly examine the effectiveness or pharmacological mechanism of Sac/Val in patients with CTRCD.

This study is subject to several limitations. Future research is required to establish the generalizability of the findings in a murine model to human subjects. Moreover, a deeper understanding of anthracycline-induced cardiomyopathy could be achieved through experimentation with human cardiomyocyte models. Additionally, the distinctive dual neuroendocrine regulatory mechanism of Sac/Val was characterized

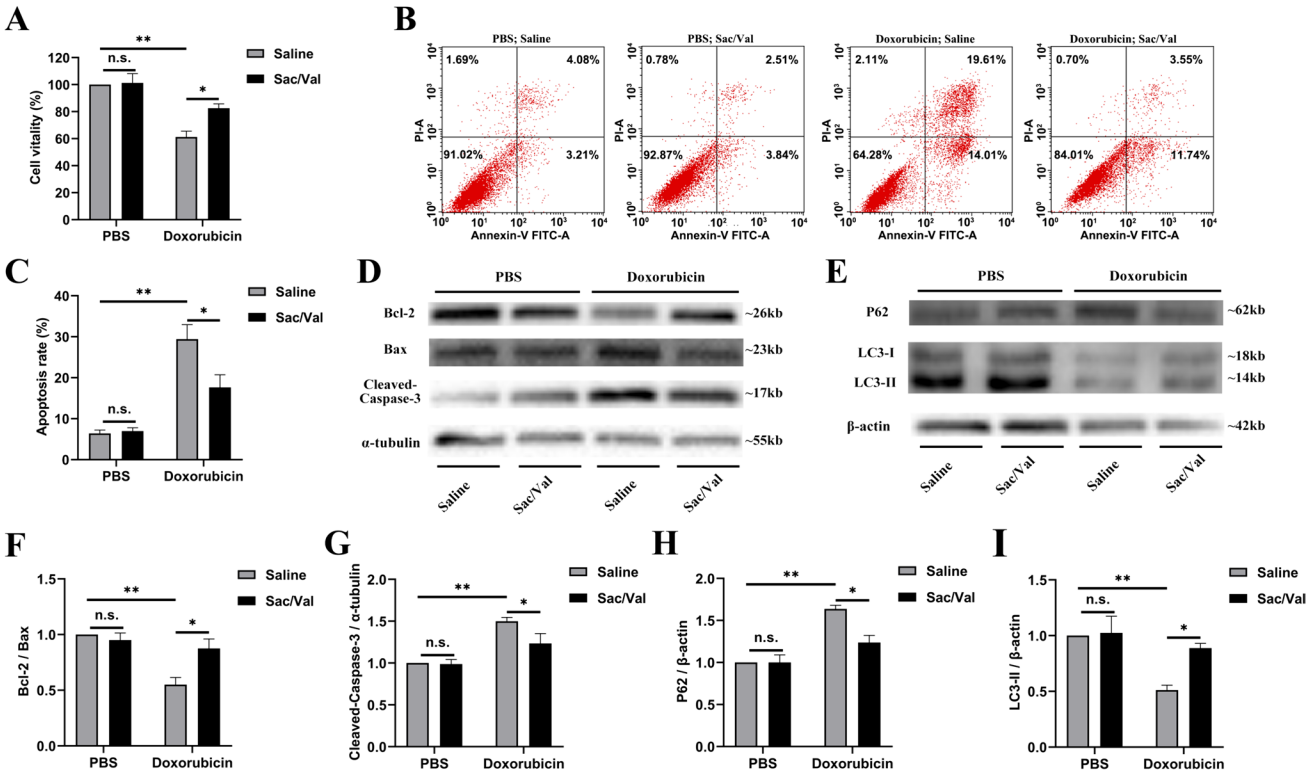

Fig. 10 Sac/Val treatment defended against DOX-induced apoptosis and autophagy inhibition in primary cardiomyocytes. For Sac/Val pre-treatment following DOX-induced cardiomyocyte toxicity, NRVMs were pre-treated with 10 μM and 20 μM each of valsartan and LCZ696 for 12 h and then treated with 5 μM of DOX for 6 h. An equal volume of PBS was incubated with NRVMs for 12 h in the CONTROL and Sac/Val group. **A** The cell viability was measured by cell counting kit-8. Compared to that in controls, the viability of cardiomyocytes significantly decreased after DOX stimulation, which was partially restored by Sac/Val treatment. **B**, **C** The apoptosis in different treatment groups was detected by flow cytometry and corresponding statistic analysis. Compared to that in controls, the apoptosis level of primary cardiomyocytes significantly increased after DOX stimulation, which was partially reversed by Sac/Val treatment. **D** Representative western blots of Bcl-2, Bax, and cleaved Caspase-3 protein in primary cardiomyocytes from the different groups. The α-tubulin was used as a loading control. **E** Representative western blots of P62 and LC3 protein in primary cardiomyocytes from the different groups. The β-actin was used as a loading control. **F**, **G** Corresponding densitometric analysis of blots in **D**. Compared to that in controls, the protein expression level of cleaved Caspase-3 significantly increased, the ratio of Bcl-2/Bax significantly decreased, in primary cardiomyocytes after DOX stimulation, which was partially restored by Sac/Val treatment. **H**, **I** Corresponding densitometric analysis of blots in **E**. Compared to that in controls, the protein expression level of P62 significantly increased, of LC3-II significantly decreased in primary cardiomyocytes after DOX stimulation, which was partially reversed by Sac/Val treatment. The cell experiment was repeated independently for three times. The data are represented as the means ± SE; $^{*}P < 0.05$, $^{**}P < 0.01$

by the inhibition of neprilysin by sacubitril, and the blockade of AT1R by valsartan resulting in the inhibition of the renin–angiotensin–aldosterone system [7–9]. The aforementioned pharmacologic action exhibited a notable distinction from conventional therapy approaches, such as ACEIs. For all this, the lack of comparison between Sac/Val and valsartan in the experiments prevents a definitive conclusion regarding the potential roles of sacubitril and valsartan separately to the observed beneficial effects.

Conclusion

This study advanced our understanding of the molecular pathways involved in anthracycline-induced cardiomyopathy. The administration of Sac/Val was shown to alleviate myocardial inflammation, fibrosis, apoptosis, enhance autophagy, and improve cardiac function in mice with

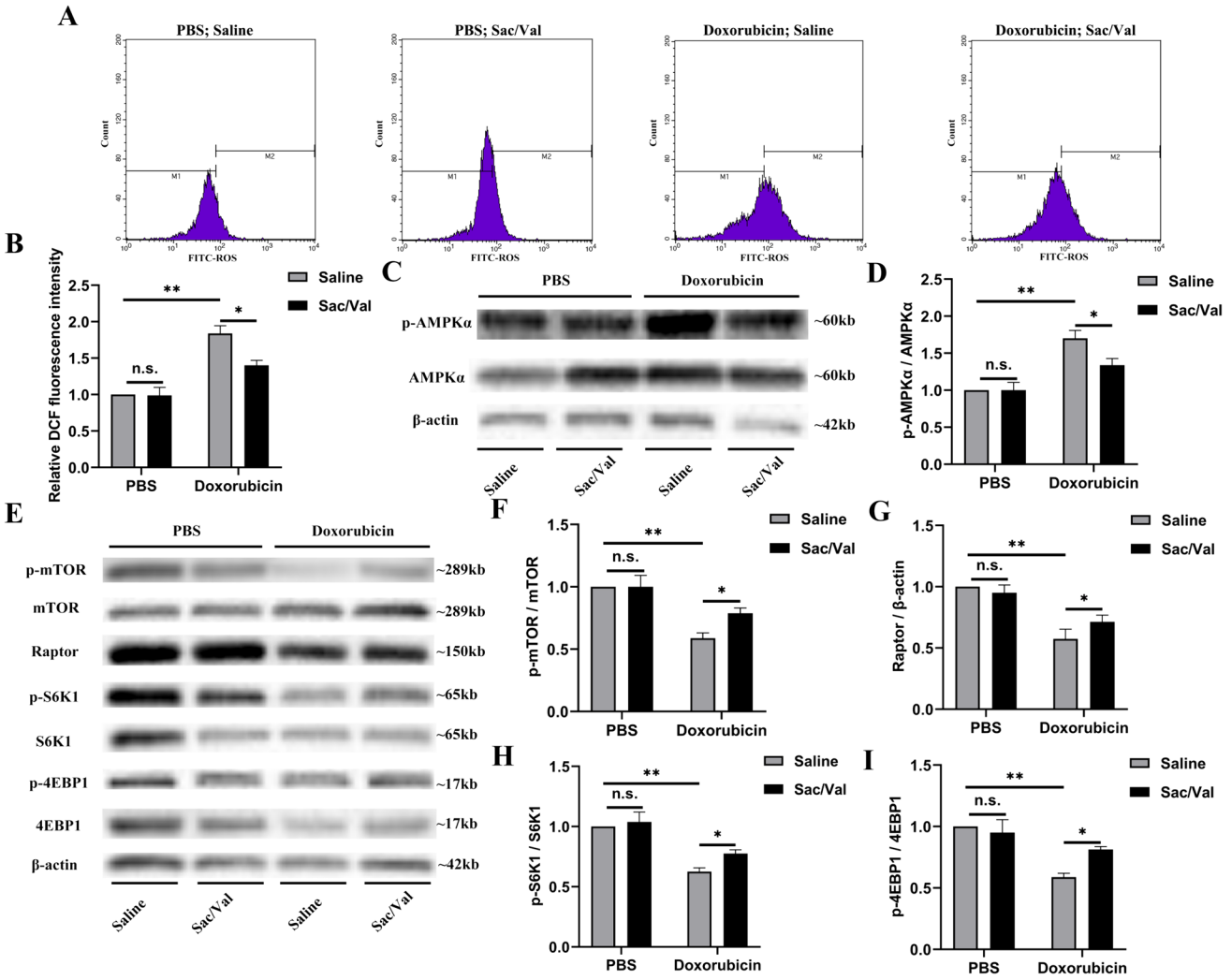

Fig. 11 Sac/Val treatment defended against DOX-induced apoptosis and autophagy inhibition via regulating the AMPKα–mTORC1 signaling pathway. **A**, **B** Intracellular ROS production in primary cardiomyocytes was detected with DCF-DA reagent and corresponding statistic analysis. Compared to that in controls, ROS levels significantly increased after DOX stimulation for 24 h in primary cardiomyocytes, which was decreased by pre-incubation with Sac/Val. **C**, **D** Representative blots of p-AMPKα and AMPKα in DOX-stimulated primary cardiomyocytes and corresponding densitometric analysis. The β-actin was used as a loading control. DOX stimulation exhibited an up-regulated protein expression level of p-AMPKα in primary cardiomyocytes, which was partly reversed by Sac/Val treatment. **E**–**I** Representative blots of p-mTOR (Ser2448), Raptor, p-S6K1 (Thr389), and p-4EBP1 (Thr37/46) in DOX-stimulated primary cardiomyocytes and corresponding densitometric analysis. The β-actin was used as a loading control. Compared to that in controls, the protein expression levels of p-mTOR (Ser2448), Raptor, p-S6K1 (Thr389), and p-4EBP1 (Thr37/46) were significantly decreased after DOX stimulation in primary cardiomyocytes, which was partly restored by Sac/Val treatment. The cell experiment was repeated independently for three times. The data are represented as the means ± SE; $*P < 0.05$, $**P < 0.01$

DOX-induced cardiotoxicity by reducing oxidative stress and regulating the AMPKα–mTORC1 signaling pathway.

Supplementary Information The online version contains supplementary material available at https://doi.org/10.1007/s11010-024-05117-7.

Acknowledgements None.

Author contributions (I) Conception and design: Weiwei Wang and Xinghe Lin; (II) Administrative support: Xinghe Lin; (III) Provision of study materials: Li Lin; (IV) Collection and assembly of data: Feng Hu and Xiaoxia Qiu; (V) Data analysis and interpretation: Senbo Yan; (VI) Manuscript writing: Feng Hu and Senbo Yan; (VII); Final approval of manuscript: All authors.

Funding This study was supported by grants from the talent start-up capital program of Fujian Medical University Union Hospital (2023XH027), the science and technology innovation joint fund project of Fujian Provincial Science and Technology Department (2023Y9183), the Fujian Provincial Natural Science Foundation.

Data availability No datasets were generated or analysed during the current study.

Declarations

Conflict of interest The authors declare no competing interests.

References

1. Michel L, Schadendorf D, Rassaf T (2020) Oncocardiology: new challenges, new opportunities. Herz 45:619–625
2. Cardinale D, Colombo A, Bacchiani G, Tedeschi I, Meroni CA, Veglia F, Civelli M, Lamantia G, Colombo N, Curigliano G, Fiorentini C, Cipolla CM (2015) Early detection of anthracycline cardiotoxicity and improvement with heart failure therapy. Circulation 131:1981–1988
3. Bowles EJ, Wellman R, Feigelson HS, Onitilo AA, Freedman AN, Delate T, Allen LA, Nekhlyudov L, Goddard KA, Davis RL, Habel LA, Yood MU, McCarty C, Magid DJ, Wagner EH (2012) Risk of heart failure in breast cancer patients after anthracycline and trastuzumab treatment: a retrospective cohort study. J Natl Cancer Inst 104:1293–1305
4. Yoodee J, Sookprasert A, Sanguanboonyaphong P, Chanthawong S, Seateaw M, Subongkot S (2021) An exploration of heart failure risk in breast cancer patients receiving anthracyclines with or without trastuzumab in Thailand: a retrospective study. Clin Pract 11:484–493
5. Saleh Y, Abdelkarim O, Herzallah K, Abela GS (2021) Anthracycline-induced cardiotoxicity: mechanisms of action, incidence, risk factors, prevention, and treatment. Heart Fail Rev 26:1159–1173
6. Cardinale D, Colombo A, Lamantia G, Colombo N, Civelli M, De Giacomi G, Rubino M, Veglia F, Fiorentini C, Cipolla CM (2010) Anthracycline-induced cardiomyopathy: clinical relevance and response to pharmacologic therapy. J Am Coll Cardiol 55:213–220
7. Docherty KF, Vaduganathan M, Solomon SD, McMurray JJV (2020) Sacubitril/valsartan: neprilysin inhibition 5 years after PARADIGM-HF. JACC Heart Failure 8:800–810
8. Pontremoli R, Borghi C, Perrone FP (2021) Renal protection in chronic heart failure: focus on sacubitril/valsartan. Eur Heart J Cardiovasc Pharmacother 7:445–452
9. McMurray JJ, Packer M, Desai AS, Gong J, Lefkowitz MP, Rizkala AR, Rouleau JL, Shi VC, Solomon SD, Swedberg K, Zile MR (2014) Angiotensin-neprilysin inhibition versus enalapril in heart failure. N Engl J Med 371:993–1004
10. Duraes AR, de Souza Lima Bitar Y, Neto MG, Mesquita ET, Chan JS, Tse G, Liu T, Bocchi EA, Biondi-Zoccai G, Roever L (2022) Effectiveness of sacubitril-valsartan in patients with cancer therapy-related cardiac dysfunction: a systematic review of clinical and preclinical studies. Minerva Med 113:551–557
11. Xia Y, Chen Z, Chen A, Fu M, Dong Z, Hu K, Yang X, Zou Y, Sun A, Qian J, Ge J (2017) LCZ696 improves cardiac function via alleviating Drp1-mediated mitochondrial dysfunction in mice with doxorubicin-induced dilated cardiomyopathy. J Mol Cell Cardiol 108:138–148
12. Dindaş F, Güngör H, Ekici M, Akokay P, Erhan F, Doğduş M, Yılmaz MB (2021) Angiotensin receptor-neprilysin inhibition by sacubitril/valsartan attenuates doxorubicin-induced cardiotoxicity in a pretreatment mice model by interfering with oxidative stress, inflammation, and Caspase 3 apoptotic pathway. Anatol J Cardiol 25:821–828
13. Boutagy NE, Feher A, Pfau D, Liu Z, Guerrera NM, Freeburg LA, Womack SJ, Hoenes AC, Zeiss C, Young LH, Spinale FG, Sinusas AJ (2020) Dual angiotensin receptor-neprilysin inhibition with sacubitril/valsartan attenuates systolic dysfunction in experimental doxorubicin-induced cardiotoxicity. JACC CardioOncol 2:774–787
14. Kim BS, Park IH, Lee AH, Kim HJ, Lim YH, Shin JH (2022) Sacubitril/valsartan reduces endoplasmic reticulum stress in a rat model of doxorubicin-induced cardiotoxicity. Arch Toxicol 96:1065–1074
15. Miyoshi T, Nakamura K, Amioka N, Hatipoglu OF, Yonezawa T, Saito Y, Yoshida M, Akagi S, Ito H (2022) LCZ696 ameliorates doxorubicin-induced cardiomyocyte toxicity in rats. Sci Rep 12:4930
16. Asselin CY, Lam A, Cheung DYC, Eekhoudt CR, Zhu A, Mittal I, Mayba A, Solati Z, Edel A, Austria JA, Aukema HM, Ravandi A, Thliveris J, Singal PK, Pierce GN, Niraula S, Jassal DS (2020) The cardioprotective role of flaxseed in the prevention of doxorubicin- and trastuzumab-mediated cardiotoxicity in C57BL/6 Mice. J Nutr 150:2353–2363
17. Yu W, Qin X, Zhang Y, Qiu P, Wang L, Zha W, Ren J (2020) Curcumin suppresses doxorubicin-induced cardiomyocyte pyroptosis via a PI3K/Akt/mTOR-dependent manner. Cardiovasc Diagn Ther 10:752–769
18. Nicol M, Sadoune M, Polidano E, Launay JM, Samuel JL, Azibani F, Cohen-Solal A (2021) Doxorubicin-induced and trastuzumab-induced cardiotoxicity in mice is not prevented by metoprolol. ESC Heart Fail 8:928–937
19. Hu F, Lin C (2024) TRPM2 knockdown attenuates myocardial apoptosis and promotes autophagy in HFD/STZ-induced diabetic mice via regulating the MEK/ERK and mTORC1 signaling pathway. Mol Cell Biochem. https://doi.org/10.1007/s11010-024-04926-0
20. Fang X, Wang H, Han D, Xie E, Yang X, Wei J, Gu S, Gao F, Zhu N, Yin X, Cheng Q, Zhang P, Dai W, Chen J, Yang F, Yang HT, Linkermann A, Gu W, Min J, Wang F (2019) Ferroptosis as a target for protection against cardiomyopathy. Proc Natl Acad Sci U S A 116:2672–2680
21. Tadokoro T, Ikeda M, Ide T, Deguchi H, Ikeda S, Okabe K, Ishikita A, Matsushima S, Koumura T, Yamada KI, Imai H, Tsutsui H (2020) Mitochondria-dependent ferroptosis plays a pivotal role in doxorubicin cardiotoxicity. JCI Insight 5:e132747
22. Tewey KM, Rowe TC, Yang L, Halligan BD, Liu LF (1984) Adriamycin-induced DNA damage mediated by mammalian DNA topoisomerase II. Science 226:466–468
23. Zhang S, Liu X, Bawa-Khalfe T, Lu LS, Lyu YL, Liu LF, Yeh ET (2012) Identification of the molecular basis of doxorubicin-induced cardiotoxicity. Nat Med 18:1639–1642
24. Willis MS, Parry TL, Brown DI, Mota RI, Huang W, Beak JY, Sola M, Zhou C, Hicks ST, Caughey MC, D'Agostino RB Jr, Jordan J, Hundley WG, Jensen BC (2019) Doxorubicin exposure causes subacute cardiac atrophy dependent on the striated muscle-specific ubiquitin ligase MuRF1. Circ Heart Fail 12:e005234

25. Jiang T, Wang M, Zhang N, Dong Q, Tang X (2023) Identification and protection of early cardiotoxicity in acute myeloid leukemia patients undergoing transplantation. Hematology 28:2239569
26. Alshammari A, Qasem BA, Almatrafi NA, Alharbi LM, Alhuthali AA, Khobrani AA, Alnuhait M (2024) Case series: sacubitril/valsartan role for chemotherapy-induced cardiotoxicity: an in-depth investigation in Saudi Arabia. Int Med Case Rep J 17:35–41
27. Bell E, Desuki A, Karbach S, Göbel S (2022) Successful treatment of doxorubicin-induced cardiomyopathy with low-dose sacubitril/valsartan: a case report. Eur Heart J Case Rep 6:ytac396
28. Sheppard CE, Anwar M (2019) The use of sacubitril/valsartan in anthracycline-induced cardiomyopathy: a mini case series. J Oncol Pharm Pract 25:1231–1234
29. Canale ML, Coviello K, Solarino G, Del Meglio J, Simonetti F, Venturini E, Camerini A, Maurea N, Bisceglia I, Tessa C, Casolo G (2022) Case series: recovery of chemotherapy-related acute heart failure by the combined use of sacubitril valsartan and wearable cardioverter defibrillator: a novel winning combination in cardio-oncology. Front Cardiovasc Med 9:801143
30. Martín-Garcia A, López-Fernández T, Mitroi C, Chaparro-Muñoz M, Moliner P, Martin-Garcia AC, Martinez-Monzonis A, Castro A, Lopez-Sendon JL, Sanchez PL (2020) Effectiveness of sacubitril-valsartan in cancer patients with heart failure. ESC Heart Fail 7:763–767
31. De Vecchis R, Paccone A (2020) A case series about the favorable effects of sacubitril/valsartan on anthracycline cardiomyopathy. SAGE Open Med Case Rep. https://doi.org/10.1177/2050313X20952189
32. Martín-García A, Díaz-Peláez E, Martín-García AC, Sánchez-González J, Ibáñez B, Sánchez PL (2020) Myocardial function and structure improvement with sacubitril/valsartan in cancer therapy-induced cardiomyopathy. Rev Esp Cardiol (Engl Ed) 73:268–269
33. Gregorietti V, Fernandez TL, Costa D, Chahla EO, Daniele AJ (2020) Use of sacubitril/valsartan in patients with cardio toxicity and heart failure due to chemotherapy. Cardiooncology 6:24
34. Ajoolabady A, Chiong M, Lavandero S, Klionsky DJ, Ren J (2022) Mitophagy in cardiovascular diseases: molecular mechanisms, pathogenesis, and treatment. Trends Mol Med 28:836–849
35. Wang L, Zhao D, Tang L, Li H, Liu Z, Gao J, Edin ML, Zhang H, Zhang K, Chen J, Zhu X, Wang D, Zeldin DC, Hammock BD, Wang J, Huang H (2021) Soluble epoxide hydrolase deficiency attenuates lipotoxic cardiomyopathy via upregulation of AMPK-mTORC mediated autophagy. J Mol Cell Cardiol 154:80–91